

Highly Ordered Protein Nanorings Designed by Accurate Control of Glutathione S-Transferase Self-Assembly

Yushi Bai,[†] Quan Luo,[†] Wei Zhang,[†] Lu Miao,[†] Jiayun Xu,[†] Hongbin Li,[‡] and Junqiu Liu^{*†}

[†]State Key Laboratory of Supramolecular Structure and Materials, College of Chemistry, Jilin University, Changchun 130012, China

[‡]Department of Chemistry, University of British Columbia, Vancouver, British Columbia, Canada V6T 1Z1

S Supporting Information

ABSTRACT: Protein self-assembly into exquisite, complex, yet highly ordered architectures represents the supreme wisdom of nature. However, precise manipulation of protein self-assembly behavior *in vitro* is a great challenge. Here we report that by taking advantage of the cooperation of metal-ion-chelating interactions and non-specific protein–protein interactions, we achieved accurate control of the orientation of proteins and their self-assembly into protein nanorings. As a building block, we utilized the C_2 -symmetric protein sjGST-2His, a variant of glutathione S-transferase from *Schistosoma japonicum* having two properly oriented His metal-chelating sites on the surface. Through synergic metal-coordination and non-covalent interactions, sjGST-2His self-assembled in a fixed bending manner to form highly ordered protein nanorings. The diameters of the nanorings can be regulated by tuning the strength of the non-covalent interaction network between sjGST-2His interfaces through variation of the ionic strength of the solution. This work provides a *de novo* design strategy that can be applied in the construction of novel protein superstructures.

Proteins are nature's most sophisticated building blocks for constructing cellular machines and performing myriad functions because of their inherent nature of spatial and functional diversity. Following the wisdom of nature, to fabricate protein self-assemblies with dominant advantages such as biocompatibility, biodegradability, structural durability, and functional versatility represents a significant area of research. However, it is a challenge to control the self-assembly behavior of proteins because of the complicated, heterogeneous protein surfaces, which can interact with each other in unpredictable ways. Some typical interactions, such as coiled-coil interactions,¹ metal-mediated interactions,² host–guest interactions,³ chemical cross-links,⁴ hydrophobic interactions,⁵ sulfide bonds,⁶ electrostatic interactions,⁷ and genetic fusion of self-associating protein domains,⁸ have been adopted in the fabrication of protein self-assemblies. In recent years, a new approach for the construction of accurately controlled protein self-assemblies through computational modeling of the weak non-covalent interactions on extensive protein surfaces has been developed.⁹ The former strategies usually do not incorporate nonspecific protein–protein interactions as a design element, whereas latter strategy requires tremendous

effort to model multi-non-specific protein–protein interactions on protein surfaces. Inspired by these efforts, here we report a *de novo* design strategy that combines the above two design concepts to exert accurate control of protein self-assembly behavior and guide their “growth” into highly ordered protein nanorings.

To construct self-assembled protein nanorings, we chose glutathione S-transferase (GST) as the building block. GST from *Schistosoma japonicum* (sjGST) is a natural homodimer that is very stable and class-specific, with the two subunits non-covalently bonded to each other and related by a twofold axis (C_2 symmetry).¹⁰ This existing symmetry provides the feasibility of constructing extended protein nanostructures. We previously proved that sjGST variants with a His tag or an FGG tag attached to the N-terminus can act as good building blocks for the construction of one-dimensional (1D) protein nanowires.^{11,12} Although those studies showed the successful assembly of sjGSTs into relatively simple 1D nanostructures, the design of novel, highly ordered architectures remains a great challenge.

We endeavored to exert accurate control of the sjGST self-assembly behavior to guide their growth in a fixed bending direction, leading finally to nanorings. To fulfill this purpose, we chose metal coordination, highlighted with the property of directionality, as our driving force. We noticed that the special C_2 symmetry of sjGST and the relative location of binding sites are key spatial geometrical elements that define the final assembled structure. According to previous work,^{11,12} when binding sites are located on the C_2 axis, sjGST variants readily assemble into protein nanowires. We wondered whether we could design two chelating sites located on the “shoulders” of the variants to form a big “V” shape from the side view, perpendicular to the C_2 axis of the dimers; this special relative orientation of the two metal chelating sites should favor the formation of protein nanorings.

The design of the chelating sites was challenging. The sjGST derivative should feature three key elements: (1) The chelating sites should protrude from the sjGST surface. sjGST is a relatively complicated protein with a rough surface, so the chelating sites should not be buried in the crevices on the surfaces to coordinate with metal ions, and the interfaces where chelating sites are located should be complementary to form stable self-assemblies (Figure S1a in the Supporting Information). (2) The relative spatial location of the chelating sites

Received: June 3, 2013

Published: July 18, 2013

must feature a proper orientation to form a “V” shape. (3) The distance between two His sites should be appropriate to form a bishistidine (bis-His) clamp. After carefully investigating the protein surface, we found that position 137 satisfies these conditions. Mutation of Cys137, which is just abreast with the endogenous His138, into a His residue would form a perfect bis-His metal-binding site, and the resulting variant dimer should satisfy the above three requirements (Figure S1b) and feature the possible trend to assemble into nanorings (Figure S1c). However, because proteins are such complicated building blocks with soft surfaces and sophisticated 3D structures, the proper orientation of the chelating sites alone may not be enough to exert accurate control over the self-assembly modes of sjGST-2His dimers. We tried to find a synergic interaction to cooperate with metal–protein coordination to exert accurate control of the protein self-assembly. In this situation, the non-covalent protein–protein interactions that play a pivotal role¹³ in the determination of the assembly behavior of proteins were studied to obtain a full understanding of the assembly details and an accurate prediction of the final structure.

To investigate the non-covalent protein–protein interactions between the sjGST variants’ surfaces, we performed calculations on all of the possible low-energy docking models of two sjGST variants. Among all the possible docking patterns, we found our chelating sites to be located on the interfaces under the magenta–green mode (Figure S2). The metal-coordination forces made this docking model “defeat” other possible docking models to be “specific” in this metal-coordination system. The relative location of two dimers under this mode should decide the assembly details. In our investigation, this mode was stabilized by a non-covalent interactions network consisting mainly of an electrostatic forces network (Asp120, Glu127, Lys130, Glu133, Asp134, and Arg41) and one hydrogen bond (Arg41, Ser123); the main residues are labeled in Figure 1. The investigation of nonspecific protein–protein interactions enriched our design of protein nanorings by bringing the 3D structures of sjGST-2His into our sight and provided the relative location of the two bis-His binding sites.

Given the spatial information concerning the two metal coordinating sites, we chose Ni²⁺ as the chelating metal ion because its stereochemical preference in solvent at low concentration¹⁴ exhibited a perfect match with the relative locations of the two bis-His clamps in this special magenta–green mode (Figure 1). Ni²⁺, which has been widely applied in Ni-NTA columns, has a high binding affinity for bis-His chelating sites and exhibits rapid ligand exchange, allowing our target nanoring to outcompete other kinetically formed structures. The nanoring formation process is illustrated in Figure 1. Driven by metal coordination, the proteins are bound together, and the interfaces are allowed to be “pulled” tightly by non-covalent interactions to form the most stable structure under thermodynamic control. Along with the growth of protein aggregates, the assembly started to exhibit a bending trend and eventually grow into a nanoring.

Four rounds of site-directed mutagenesis were carried out: besides mutating Cys137 into His to form the bis-His metal-chelating sites, the three Cys residues at positions 84, 168, and 177 were mutated into Ser to avoid unspecific metal coordination at neutral pH. The purity and verification of the mutations of the resulting sjGST variant, sjGST-2His, were characterized by SDS-PAGE (Figure S3) and MALDI-TOF mass spectrometry (Figure S4).

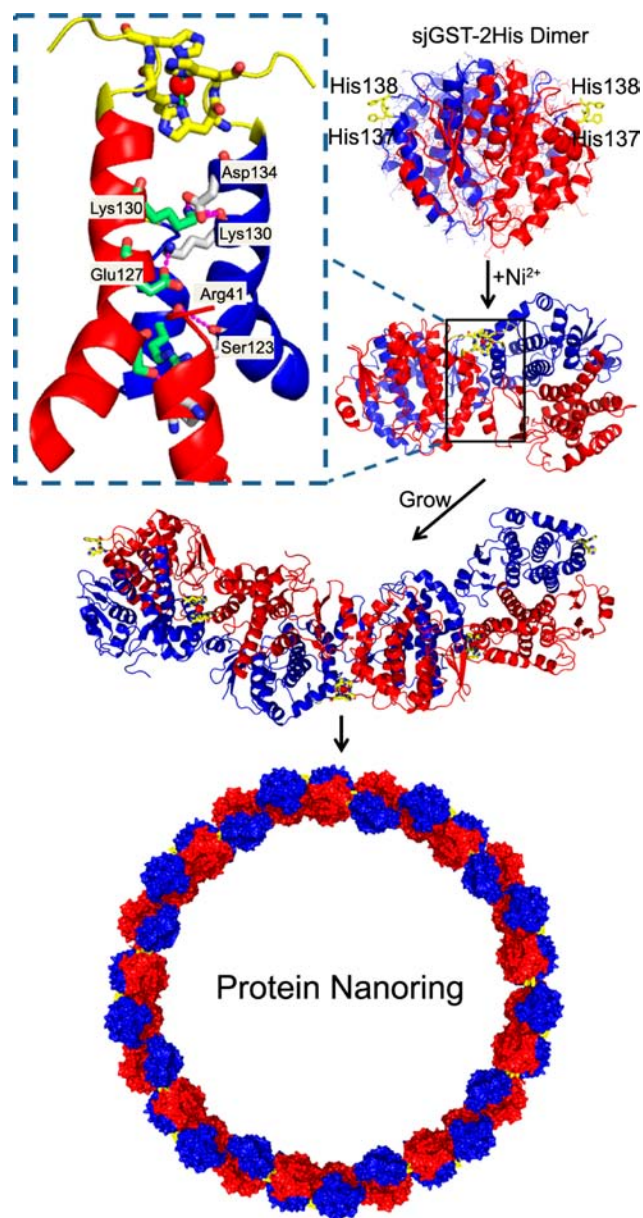


Figure 1. Schematic representation of the formation of protein nanorings through Ni²⁺–His coordination.

Dynamic light scattering (DLS) measurements gave a preliminary characterization of the formation of sjGST-2His aggregates upon Ni²⁺ addition (Figure S5). The trend of increasing hydrodynamic radius with the addition of Ni²⁺ suggested that Ni–His coordination can force sjGST-2His to assemble into aggregates. Circular dichroism (CD) was utilized to evaluate the effect of the introduction of chelating sites (Figure S6) and addition of Ni²⁺ (Figure S7) on the secondary structure of wild-type sjGST. No significant transition of the secondary structure was observed in the CD spectra, suggesting that the mutation of sjGST and the formation of protein self-assemblies did not disarrange the secondary structure of sjGST. In view of the fact that sjGST is a natural enzyme, the construction of sjGST-2His self-assemblies also bears the potential for building functional biomaterials.

Tapping-mode atomic force microscopy (AFM) was used to investigate the morphology of the sjGST-2His self-assemblies and provide a direct characterization of the “nanorings”. Freshly

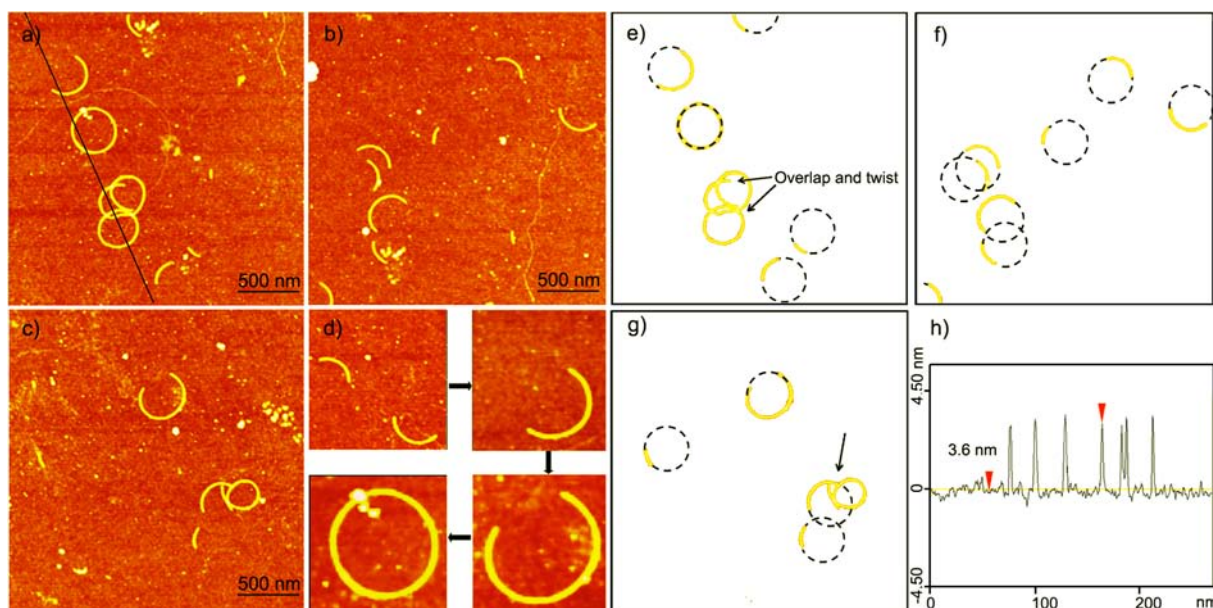


Figure 2. AFM characterization of protein nanorings. (a–c) AFM images of protein nanorings formed in pure water under Ni^{2+} coordination at a $\text{Ni}^{2+}/\text{sjGST-2His}$ ratio of 1:1. (d) Different stages of nanoring growth. (e–g) Following the curvature of the protein half-rings in (a–c), the “full nanorings” with same growing tendency were utilized to evaluate the diameters of the nanorings. Overlap and twisting of two collided “growing arcs” in (e) and (g) are indicated with arrows. (h) Height profile along the black line in (a).

prepared sjGST-2His was dissolved in pure water at a concentration of $0.1 \mu\text{M}$, and 1 equiv of Ni^{2+} was added into the solution. After the mixture was allowed to incubate overnight at 4°C , a $10 \mu\text{L}$ aliquot of the sample was deposited onto freshly cleaved silicon wafer, incubated for 5 min, and dried with nitrogen.

The AFM data clearly show the formation of highly ordered protein nanorings and half-rings under different growing periods (Figure 2a–c). Different periods of protein nanorings were extracted out to elucidate that the formation of protein nanorings proceeded by a bottom-up strategy (Figures 2d and S8). Through following the curvature of the arcs in Figure 2a–c we were able to obtain the final ring structure (Figure 2e–g). We observed that all of the predicted nanorings had the same diameter ($367 \pm 10 \text{ nm}$), which means that if not disturbed, all of the half-rings adopted an identical curvature and would grow in the same way. However, when they collided with each other in the process of growth, twisting and overlap of “growing arcs” occurred (Figure 2e,g). This softness and flexibility suggested a special property belonging to protein assemblies. The height of the assemblies spread evenly, which is equal to the height of a single dimer on the sample, was revealed to be 3.6 nm (Figure 2h). The kinetics of the bottom-up assembly process were also monitored by DLS (Figure S9). The above results clearly recapitulated the designed nanorings, which confirmed that our combined consideration of the steric orientation of metal-chelating sites and nonspecific protein–protein interactions can give an accurate prediction of the final assemblies.

After the successful construction of protein nanorings in pure water, we attempted to regulate the diameter of the nanorings. According to the concept that sjGST-2His nanorings are a synergic result of metal-coordination interactions and mainly electrostatic non-covalent interactions, the regulation of the non-covalent interactions could act as a good breakthrough point. At high ionic strength, the non-covalent interactions between protein interfaces should be weakened, resulting in a greater distance between sjGST-2His dimers and thus an

increased curvature of the assemblies, which may lead to the formation of “small” rings (Figure S10). AFM data indeed revealed that sjGST-2His assembled into small rings when transferred to 20 mM Tris buffer (pH 7.0) with 30 mM NaCl (Figure 3a–c). The diameters of the small rings were measured to be $96 \pm 5 \text{ nm}$. The height of the assembly in buffer was identical to that in pure water (Figure 3d).

Comparative analysis of the “big” and “small” rings indicated that the big rings in water packed so densely that no single dimers could be told apart and the borderline between

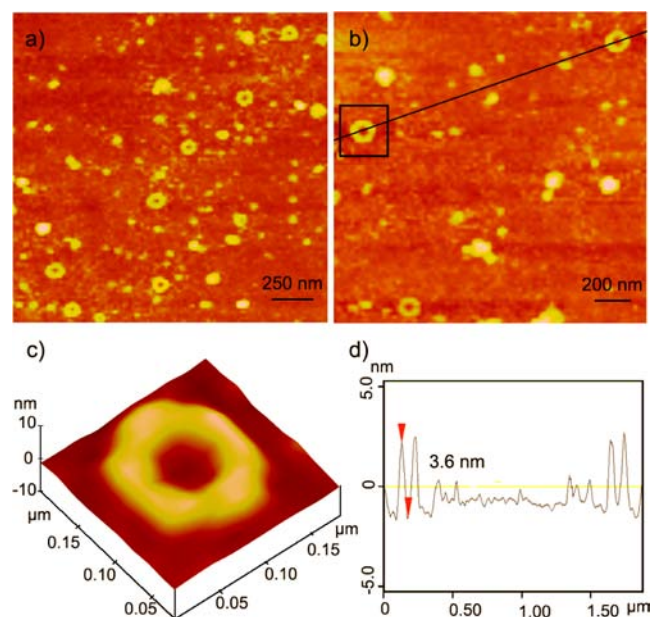


Figure 3. AFM characterization of small rings in 20 mM Tris (pH 7.0) with 30 mM NaCl. (a, b) small rings formed in buffer with 30 mM NaCl. (c) Enlarged 3D image of the single nanoring in the black box in (b). (d) Height profile along the black line in (b).

neighboring dimers was smooth. In contrast, for the small rings in buffer, dimers were loosely bound with a rugged borderline, and the junctions of the dimers could be seen (Figure S11). This observation was consistent with our proposed mechanism that altering the ionic strength would tune the non-covalent interaction network, providing further control over the assembly behavior of sjGST-2His. In fact, by altering the ionic strength of the solution, a series of self-assembled protein nanorings with different diameters were also obtained (Figure S12). The diameters of the protein nanorings decreased with the salt concentration, which ranged from 10 mM to 50 mM. At higher salt concentrations (>50 mM), sjGST-2His totally assembled into small, irregular aggregates.

The formation of small rings and the regulation of the protein nanoring diameter provides solid evidence that validates our design of protein nanorings under the synergic action of metal–protein coordination and nonspecific protein–protein interactions.

A major hurdle to be overcome in exerting accurate control over protein self-assemblies is that protein surfaces indeed provide complicated ligands that can interact with each other and always assemble in ways that are hard to predict.¹⁵ Our study provides a solution to this problem through the cooperation of directional metal–protein coordination and nonspecific protein–protein interactions, which enables accurate control of protein self-assembly behavior. Thus, novel highly ordered protein structures can be designed and constructed through a bottom-up strategy. Our study represents an important step toward the full control of proteins and paves the way for the construction of more grand protein superstructures with higher dimensions and more sophisticated configurations.

■ ASSOCIATED CONTENT

■ Supporting Information

Design of the sjGST variant, calculation of protein–protein interactions, materials and methods for protein expression/purification/characterization, experimental and analytical details of CD measurements, DLS and AFM characterization, and mechanism for small ring formation. This material is available free of charge via the Internet at <http://pubs.acs.org>.

■ AUTHOR INFORMATION

Corresponding Author

junqiuliu@jlu.edu.cn

Notes

The authors declare no competing financial interest.

■ ACKNOWLEDGMENTS

We acknowledge financial support from the National Natural Science Foundation of China (21234004, 91027023, 21221063, 21004028) and the 111 Project (B06009).

■ REFERENCES

- (1) (a) Harbury, P. B.; Plecs, J. J.; Tidor, B.; Alber, T.; Kim, P. S. *Science* **1998**, *282*, 1462. (b) Zaccai, N. R.; Chi, B.; Thomson, A. R.; Boyle, A. L.; Bartlett, G. J.; Bruning, M.; Linden, N.; Sessions, R. B.; Booth, P. J.; Brady, R. L.; Woolfson, D. N. *Nat. Chem. Biol.* **2011**, *7*, 935. (c) Minten, I. J.; Hendriks, L. J. A.; Nolte, R. J. M.; Cornelissen, J. J. L. M. *J. Am. Chem. Soc.* **2009**, *131*, 17771.
- (2) (a) Brodin, J. D.; Ambroggio, X. L.; Tang, C. Y.; Parent, K. N.; Baker, T. S.; Tezcan, F. A. *Nat. Chem.* **2012**, *4*, 375. (b) Salgado, E. N.; Faraone-Mennella, J.; Tezcan, F. A. *J. Am. Chem. Soc.* **2007**, *129*,

13374. (c) Radford, R. J.; Tezcan, F. A. *J. Am. Chem. Soc.* **2009**, *131*, 9136.

- (3) (a) Carlson, J. C. T.; Jena, S. S.; Flenniken, M.; Chou, T. F.; Siegel, R. A.; Wagner, C. R. *J. Am. Chem. Soc.* **2006**, *128*, 7630. (b) Kitagishi, H.; Oohora, K.; Yamaguchi, H.; Sato, H.; Matsuo, T.; Harada, A.; Hayashi, T. *J. Am. Chem. Soc.* **2007**, *129*, 10326. (c) Kitagishi, H.; Kakikura, Y.; Yamaguchi, H.; Oohora, K.; Harada, A.; Hayashi, T. *Angew. Chem., Int. Ed.* **2009**, *48*, 1271.
- (4) Ringle, P.; Schulz, G. E. *Science* **2003**, *302*, 106.
- (5) (a) Boerakker, M. J.; Hannink, J. M.; Bomans, P. H. H.; Frederik, P. M.; Nolte, R. J. M.; Meijer, E. M.; Sommerdijk, N. A. J. M. *Angew. Chem., Int. Ed.* **2002**, *41*, 4239. (b) Boerakker, M. J.; Botterhuis, N. E.; Bomans, P. H. H.; Frederik, P. M.; Meijer, E. M.; Nolte, R. J. M.; Sommerdijk, N. A. J. M. *Chem.—Eur. J.* **2006**, *12*, 6071.
- (6) (a) Ballister, E. R.; Lai, A. H.; Zuckermann, R. N.; Cheng, Y.; Mougous, J. D. *Proc. Natl. Acad. Sci. U.S.A.* **2008**, *105*, 3733. (b) Miranda, F. F.; Iwasaki, K.; Akashi, S.; Sumitomo, K.; Kobayashi, M.; Yamashita, I.; Tame, J. R. H.; Hedde, J. G. *Small* **2009**, *5*, 2077.
- (7) (a) Chen, C. L.; Bromley, K. M.; Moradian-Oldak, J.; DeYoreo, J. J. *J. Am. Chem. Soc.* **2011**, *133*, 17406. (b) Kostiaainen, M. A.; Hiekkataipale, P.; Laiho, A.; Lemieux, V.; Seitsonen, J.; Ruokolainen, J.; Ceci, P. *Nat. Nanotechnol.* **2013**, *8*, 52.
- (8) Sinclair, J. C.; Davies, K. M.; Vénien-Bryan, C.; Noble, M. E. *Nat. Nanotechnol.* **2011**, *6*, 558.
- (9) King, N. P.; Sheffler, W.; Sawaya, M. R.; Vollmar, B. S.; Sumida, J. P.; André, I.; Gonen, T.; Yeates, T. O.; Baker, D. *Science* **2012**, *336*, 1171.
- (10) Jao, S. C.; Chen, J.; Yang, K.; Li, W. S. *Bioorg. Med. Chem.* **2006**, *14*, 304.
- (11) Zhang, W.; Luo, Q.; Miao, L.; Hou, C. X.; Bai, Y. S.; Dong, Z. Y.; Xu, J. Y.; Liu, J. Q. *Nanoscale* **2012**, *4*, 5847.
- (12) Hou, C. X.; Li, J. X.; Zhao, L. L.; Zhang, W.; Luo, Q.; Dong, Z. Y.; Xu, J. Y.; Liu, J. Q. *Angew. Chem., Int. Ed.* **2013**, *52*, 1.
- (13) Salgado, E. N.; Lewis, R. A.; Faraone-Mennella, J.; Tezcan, F. A. *J. Am. Chem. Soc.* **2008**, *130*, 6082.
- (14) Salgado, E. N.; Lewis, R. A.; Mossin, S.; Rheingold, A. L.; Tezcan, F. A. *Inorg. Chem.* **2009**, *48*, 2726.
- (15) Salgado, E. N.; Radford, R. J.; Tezcan, F. A. *Acc. Chem. Res.* **2010**, *43*, 661.